Solid Earth Discuss., 6, 2401–2422, 2014
www.solid-earth-discuss.net/6/2401/2014/
doi:10.5194/sed-6-2401-2014

Solid Earth
Discussions
Open Access

Features of the Earth surface deformations in Kamchatka peninsula and their relation with geoacoustic emission

I. A. Larionov, Yu. V. Marapulets, and B. M. Shevtsov

Institute of Cosmophysical Research and Radio Wave Propagation (FEB RAS), Paratunka
Kamchatskiy krai, Russia

Received: 7 July 2014 – Accepted: 29 July 2014 – Published: 15 August 2014

Correspondence to: Yu. V. Marapulets (marpl@ikir.ru) and I. A. Larionov (igor@ikir.ru)

Published by Copernicus Publications on behalf of the European Geosciences Union.

Abstract

The paper presents the results of investigations of deformation process in the near surface sedimentary rocks, which has been carried out in a seismically active region of Kamchatka peninsular since 2007. The peculiarity of the experiments on registration of geodeformations is the application of a laser strainmeter-interferometer constructed according to the Michelson interferometer scheme. Besides rock deformations, geoacoustic emission in the frequency range from several hertz to the first tens of kilohertz is under the investigation. Piezoceramic hydrophones installed in artificial water reservoirs are applied. It is shown that periods of primary rock compression and tension with the duration up to several months are distinguished in the geodeformation process at the observation site. During the direction change in the deformations, when geodeformation process rate grows, the increase of geoacoustic radiation is observed.

1 Introduction

Kamchatka peninsular, one of seismically active regions of the planet, is a natural test ground for investigation of seismo-tectonic process which appears as a result of stress accumulation and relaxation in the lithosphere. It is a natural geodeformation process accompanying the movement and interaction of continental and oceanic plates. The topicality of its investigation is determined by the fact, that it plays an important role in many geophysical processes which are discussed in seismology, mining and other spheres of science and engineering. Acoustic emission is elastic oscillations occurring in the result of dislocation changes in a media. They are often used to make diagnostics of deformations, since the characteristics of the excited radiation are directly associated with deformation process features. The phenomenon of acoustic emission is observed in a wide range of materials, structures and processes. The most large-scale acoustic emission is associated with seismic waves whereas the least scale level is caused by dislocation movement in crystals. Between these two types of acoustic emission

Title Page
Abstract Introduction
Conclusions References
Tables Figures
◀| |▶
◀ ▶
Back Close
Full Screen / Esc
Printer-friendly Version
Interactive Discussion

is a wide range of scales from laboratory tests and natural experiments to industrial control (Pollock, 1970, 1989). Mesoscale range, corresponding to sound vibrations, has an intermediate position according to wavelength and plays an important role in the interaction of macro and micro dislocations. Hardness of landscapes, mountain slopes, glaciers, snow covers and large technical constructions is associated with mesoscale deformation processes. Increase of regional mesoscale deformations is observed at the final stage of earthquake preparation (Agnew et al., 2003; Berardino et al., 2002; Dolgikh et al., 2007; Sasorova et al., 2008). In the result, local effects of earthquake precursors of different nature appear, including those in acoustic signals of sound range (Dolgikh et al., 2007; Gregori et al., 2005, 2010; Kuptsov, 2005; Levin et al., 2010; Morgunov et al., 1991; Paparo et al., 2002; Sasorova et al., 2008).

During the development of acoustic methods for investigation of mesoscale deformations, the principal difficulties appear due to the significant inhomogeneity of natural media and hard propagation conditions for elastic oscillations, particularly in the frequency range of the first kilohertz. Strong distortion and weakening of a signal restrict the possibilities of remote methods and require the development of distributed measuring systems applying modern data-processing technologies which have reach the required level only during the recent years. Investigation of the relation of geoacoustic emission with regional deformation disturbances needs the organization of long distributed observations, construction of specialized systems for data acquisition and processing, development of models adopted to real conditions for solving inverse problems to determine the regions of deformation disturbances.

It is reasonable to carry out investigations of mesoscale deformations in seismically active regions. Seismotectonic process is constantly going on there accompanied by stronger rock deformations, thus, stronger effects in geoacoustic emission should be registered. It is confirmed by the results of investigations in different seismically active regions (Gregori et al., 2005, 2010; Kuptsov, 2005; Levin et al., 2010; Morgunov et al., 1991; Paparo et al., 2002; Sasorova et al., 2008), where geoacoustic emission anomalies in the frequency range of the first kilohertz, which preceded strong earthquakes, were determined. The papers (Alekseev et al., 2001; Dobrovolsky, 2000; Okada, 1985; Vodinchar et al., 2007) present the models which show deformation nature of appearance of such anomalies, and the paper (Dolgikh et al., 2007) experimentally confirms the relation of geoacoustic emission anomaly with the dynamics of geodeformation process before an earthquake. Near surface sedimentary rocks, characterized by low strength and high plasticity, are the most suitable for investiagion of deformations. Even a small stress change there causes geoacoustic emission. It should be taken into account, that changes in sedimentary rock deformations may be determined both by the dynamics of a regional seismotectonic process and local peculiarities of a registration site. Rock plastic flows from near mountain slopes, soil seasonal freezing and defrosting, sharp changes of atmospheric pressure during cyclones also may contribute. In all these cases anomalous behavior of geodeformation process and geoacoustic emission response will be registered. In the present paper the authors did not aim at the classification of anomalies in deformations but they tried to analyze the peculiarities of geodeformation process registered at one measurement site within a long period of time and to determine the peculiarities of its relation with geoacoustic emission.

2 Measurement technique

A laser strainmeter-interferometer of an unequal-arm type, constructed according to the scheme of Michelson interferometer (Fig. 1) and developed at TOI FEB RAS (Dolgikh et al., 2007, 2012) is used to investigate deformations. The principle of operation of a laser strainmeter is that strainmeter basis change causes additional phase increment in a laser radiation wave. The measurement method is the following. Shift of interferometer mirrors, placed at the ends of basis l, by $\lambda/2$ value results in the change of interference pattern by one band where λ is the light wave length on which interferometer operates. Total relative shift will be equal to $\Delta l = N(\lambda/2)$, where N is the number of interference pattern bands. The capabilities of the interference method are limited by the accuracy of measurement of band shifts ΔN, which is determined by the parameter of interference pattern sharpness F_k and is characterized by the relation $F_k = \frac{\Delta\lambda}{\delta\lambda}$, i.e. it is the relation of the distance between maxima to maximum half width $\delta\lambda$.

The advantage of a laser strainmeter against a mechanic one is the absence of a mechanic sensitive element (Agnew et al., 2003; Amoruso et al., 2009; Dolgikh et al., 2012). The effect of meteorological parameter variations on the instrument is mainly the change of laser beam optical path. When a sealed or a vacuum-treated lightguide is used, the measurement accuracy of the Earth crust relative deformations for the best interferometer models is 10^{-10}–10^{-11}. Some restrictions, determined by the effect of meteorological parameter variation, are imposed on registration accuracy for the measurements carried out by "open" type strainmeters without lightguides. In terms of calculation data, a strainmeter installed in such conditions has the relative deformation measurement accuracy not less than 10^{-8}. Results of the experiments in Kamchatka show, that for the deformations of such order and more, some effects appear in sedimentary rocks when acoustic signals are generated in the frequency range from hundreds of hertz to the first ten of hilohertz (Dolgikh et al., 2007).

A laser strainmeter-interferometer was installed on the ground surface on case pipes of two five-meter dry wells 18 m spaced (interferometer measurement arm length) at "Karymshina" complex geophysical observation site in Kamchatka. Figure 1 shows its structural scheme. The interferometer measurement basis was covered from precipitations; vacuum-treated lightguide for the laser beam was not used.

The system for geoacoustic emission measurement was realized by directed broadband piezoceramic hydrophones installed in covered artificial reservoirs with the size 1 m × 1 m × 1 m (Kuptsov, 2005; Smirnov et al., 2012). The distances between the hydrophones of 5 to 50 m were chosen according to the estimation of acoustic signal attenuation in the frequency range from hundreds of hertz to the first ten of kilohertz where the maximum of geoacoustic radiation is registered. The receiving system included four hydrophones oriented downward with the diameter of receiving plate $D = 65$ mm and the length of directional diagram $\theta = \lambda/D$, where λ is radiation wave length. Structural scheme of geoacoustic emission registration system is illustrated in Fig. 2.

Continuous registration of a signal in the sound range was carried out simultaneously with digital filtration of the signal in the ranges: 0.1–10, 30–60, 70–200, 200–600, 600–2000, 2000–6500, 6500–11 000 Hz with the following collection at a second interval (Marapulets et al., 2012).

Meteorological parameters (primary wind and rain), monitored by Conrad WS 2103 digital station, affected the registered signal the most in the range up to one hundred hertz, but they did not influence the geoacoustic emission observations at higher frequencies. Anthropogenic noise (airplanes, cars and diesel generator) caused disturbances which were rather simply detected during data interpretation. To analyze the seismic state, an on-line catalogue of Kamchatka Branch of RAS Geophysical Service was used.

3 Main results and discussion

Registration of near surface sedimentary rock deformations has been carried out since 2007. An example of the data is presented in Fig. 3. Rock relative deformation ε was considered (Fig. 3a). In order to analyze its dynamics, first differences were applied. They were calculated by averaged close values of ε at a second interval. They were considered as estimations of rock deformation rate $\dot{\varepsilon}$ (Fig. 3b).

In the course if the investigation of geoacoustic emission, it was determined that anomalies in kilohertz frequency range register 1–3 days before strong earthquakes at the distances of the first hundreds of kilometers from an epicenter (Kuptsov et al., 2005). As an example, Fig. 4 illustrates nearly one day anomaly which was observed on 22–23 August 2006 before a group of 15 seismic events registered on 24 August 2006 at the distance of about 200 km. The strongest earthquake with the energy class $K = 13.8$ occurred at 21:50 UTC on 24 August 2006 at the epicentral distance of 220 km. Earthquake hypocenter coordinates are 51.01° N, 158.01° E, the depth is

40 km. In this case an emission anomaly of a complicated form was registered in which at the background of a continuous increase of acoustic noise level in kilohertz frequency ranges higher frequency quasi-periodic pulsations were observed.

The relation of geoacoustic disturbances, preceding seismic events, with geodeformation changes was under the investigation. In order to do that, a pieso-ceramic hydrophone was temporally installed in a water reservoir on the strainmeter base. In the case experiment on 1 May 2007 an anomalous deformation pattern in comparison to the levels of calm diurnal variation was registered. These sharp oscillations had quite a large amplitude of about 10^{-8} relatively the diurnal values (Fig. 5a). Such behavior of relative deformation ε lasted for about 8 h and took place 25 h before an earthquake with the energy class $K = 12.1$, which occurred on 2 May 2007 at 12:00 UTC at the epicentral distance of 154 km. Earthquake hypocenter coordinates are 52.44° N, 160.33° E, the depth is 12 km. Geoacoustic emission analysis for the same period discovered a sharp increase of acoustic pressure P_s collected on the second interval, especially in the frequency range of 2.0–6.5 kHz. Anomalous increase of the emission amplitude corresponds to the region of sharp oscillations in the deformation (Fig. 5c) which is clearly seen on the graph of its rate (Fig. 5b). The area of disturbances is marked by a rectangle (Fig. 5) and is shown in Fig. 6 in detail.

To estimate the relation between geoacoustic emission and rock deformations, cross-correlation functions (CCF) between acoustic pressure second series P_s in the range of 2.0–6.5 kHz and relative deformation ε (Fig. 7), as well as deformation rate (Fig. 8) for the period from 0 till 12 o'clock on 1 May were calculated. In the both cases CCF maximum was observed on a zero sift and was −0.53 and 0.42, correspondingly, with the significance level in the both cases not less than 0.001.

Further, the results of joint investigation of geoacoustic emission (the hydrophone is installed at the distance of 50 m from the strainmeter) and rock deformation confirmed that emission anomalies in kilohertz frequency range are observed during significant increase of deformation rate both during near surface sedimentary rock compression (Fig. 9) and tension (Fig. 10).

It is clear from the comparison of the graphs of emission and deformation rate that geoacousic disturbances occur during numerous sign-changing rock shifts of different amplitude. Relative deformations of some shifts are small enough; even at comparatively large amplitude they are not more than 10^{-8}. The data, shown in Figs. 9 and 10, were obtained during seismically calm periods when no earthquakes with the energy class $K > 10$ were registered at the distance up to 250 km.

During the data analysis for the whole period of observations since 2007, diurnal data, when registration was stopped on different technical reasons, were removed from the consideration. For this reason, during the first two years of the experiment, the period of adjustment of the measurement, it was impossible to obtain deformation long data series to estimate the annual scale pattern. During the following period the number of gaps decreased significantly and it allowed us to consider the geodeformation process behavior within long time periods.

Figure 11a shows an example of deformation change from March 2010 till February 2012. Due to considerable oscillations of deformations on the annual time scale, diurnal variations turned to be smoothed. To make objective estimations, graphs of median values and mean square deviation (MSD) of the difference between diurnal relative deformation maximal and minimal values $\Delta\varepsilon$, averaged in a week window, were calculated and plotted (Fig. 11b). Acoustic pressure pattern P_s in the range of 0.6–2 kHz, averaged in a day window, is illustrated in Fig. 11c. Due to the peculiarities of geoacoustic emission registration at “Karymshina” site, this range is weakly influenced by meteorological factors, but the disturbances of deformation nature affect it the most. Data averaging in a day window allowed us to eliminate short-term disturbances and to determine the specific level of acoustic pressure at long time intervals.

As it follows from Fig. 11, during long periods, rock primary compression or tension are observed, but the most interesting are the regions where geodeformation direction change occurred. For example, in July–November 2010 in the deformation process, the primary compression is changed by primary tension, and the median values and the MSD show average value increase and relatively average value peak in relative deformation diurnal variations. From October 2011 till February 2012 deformation direction change occurred, rock primary compression rate grew sharply as well as the intensity of relative deformation per a day. During this period the most significant amplitude disturbance of geoacoustic emission was determined. It should be noted, that such a strong compression for a short enough time period was registered for the first time.

4 Conclusions

Primary rock compression or tension, which last for several months, is observed in the deformation process, registered at the observation site in Kamchatka. Similar results were obtained in the paper (Agnew et al., 2003). It allows us to suggest that similar effects are typical for the local deformation process. Geoacoustic anomalies are mainly registered during deformation direction change when deformation process rate increases.

When deformations become more active, geoacoustic emission anomalies are observed in the form of a sharp and long increase of the level in the frequency range from hundreds of hertz to the units of kilohertz. During these periods deformation rate grows and rock slips appear which result in the generation of the emission of increased intensity. The most vividly such effects are observed at the final stage of earthquake preparation. This result agrees well with the results of mathematical models (Alekseev et al., 2001; Dobrovolsky, 2000; Okada, 1985; Vodinchar et al., 2007) and natural experiments (Agnew et al., 2003; Berardino et al., 2002; Dolgikh et al., 2007; Sasorova et al., 2008). These authors showed that amplification of deformation process occurs during earthquake preparation in the regions of their epicenters at the distance up to several hundreds of kilometers. Thus, anomalies of geoacoustic emission in the frequency range from hundreds of hertz to the units of hertz may be considered as operative precursors of strong earthquakes.

The Supplement related to this article is available online at doi:10.5194/sed-6-2401-2014-supplement.

References

Agnew, D. C. and Wyatt, F. K.: Long-base laser strainmeters: a review, Scripps institution of oceanography technical report, available at: http://repositories.cdlib.org/sio/techreport/2, 2003.

Alekseev, A. S., Belonosov, A. S., and Petrenko, V. E.: A concept of multidisciplinary earthquake prediction using an integrated precursor, Vychislitel'naya Seysmologiya, 32, 81–97, 2001.

Amoruso, A. and Crescentini, L.: The geodetic laser interferometers at Gran Sasso, Italy: recent modifications and correction for local effects, J. Geodyn., 48, 120–125, 2009.

Berardino, P., Fornaro, G., Lanari, R., and Sansosti, E.: A new algorithm for surface deformation monitoring based on small baseline differential SAR interferograms, IEEE T. Geosci. Remote, 40, 2375–2383, 2002.

Dobrovolsky, I. P.: Theory of the Earthquake Preparation, UIPE RAS, Moscow, 2000.

Dolgikh, G. I., Shvets, V. A., Chupin, V. A., Yakovenko, S. V., Kuptsov, A. V., Larionov, I. A., Marapulets, Yu. V., Shevtsov, B. M., and Shirokov, O. P.: Deformation and acoustic precursors ofearthquakes, Dokl. Earth Sci., 413, 281–285, 2007.

Dolgikh, S. G., Chupin, V. A., Shvets, V. A., and Yakovenko, S. V.: Gornotaezhnoe geophysical system, Instrum. Exp. Tech., 55, 298–299, 2012.

Gregori, G. P., Paparo, G., Poscolieri, M., and Zanini, A.: Acoustic emission and released seismic energy, Nat. Hazards Earth Syst. Sci., 5, 777–782, doi:10.5194/nhess-5-777-2005, 2005.

Gregori, G. P., Poscolieri, M., Paparo, G., De Simone, S., Rafanelli, C., and Ventrice, G.: "Storms of crustal stress" and AE earthquake precursors, Nat. Hazards Earth Syst. Sci., 10, 319–337, doi:10.5194/nhess-10-319-2010, 2010.

Kuptsov, A. V.: Changes of acoustic emission character corresponding to the final stage of seismic event development, Earth Physics, 10, 825–831, 2005.

Kuptsov, A. V., Larionov, I. A., and Shevtsov, B. M.: Peculiarities of geoacoustic emission during Kamchatka earthquake preparation, Volcanol. Seismol., 5, 45–59, 2005.

Levin, B. V., Sasorova, E. V., Borisov, S. A., and Borisov, A. S.: Estimating the Parameters of Small Earthquakes and Their Signals, J. Volcanol. Seismol., 3, 60–70, 2010.

Marapulets, Yu. V., Shevtsov, B. M., Larionov, I. A., Mishchenko, M. A., Shcherbina, A. O., and Solodchuk, A. A.: Geoacoustic emission response to deformation processes activation during earthquake preparation, Russ. J. Pac. Geol., 6, 457–464, 2012.

Morgunov, V. A., Luboshevskiy, M. N., Fabritsius, V. Z., and Fabritsius, Z. E. Geoacousic precursor of Spitak earthquake, Volcanol. Seismol., 4, 104–106, 1991.

Okada, Y.: Surface deformation due to shear and tensile faults in a half-space, B. Seismol. Soc. Am., 75, 1135–1154, 1985.

Paparo, G., Gregori, G. P., Coppa, U., De Ritis, R., and Taloni, A.: Acoustic Emission (AE) as a diagnostic tool in geophysics, Ann. Geophys.-Italy, 45, 401–416, 2002.

Pollock, A. A.: Acoustic emission, Non-Destruct. Test., 209, 639–642, 1970.

Pollock, A. A.: Acoustic emission inspection, in: Metals Handbook, Vol. 17, 278–294, 1989.

Sasorova, E. V., Levin, B. W., and Morozov, V. E.: Hydro-seismic-acoustical monitoring of submarine earthquakes preparation: observations and analysis, Adv. Geosci., 14, 99–104, doi:10.5194/adgeo-14-99-2008, 2008.

Smirnov, S. E. and Marapulets, Y. V.: Influence of a single lightning discharge on the intensity of an air electric field and acoustic emission of near-surface rocks, Solid Earth, 3, 307–311, doi:10.5194/se-3-307-2012, 2012.

Vodinchar, G. M., Perezhogin, A. S., Sagitova, R. N., and Shevtsov, B. M.: Simulation of geoacoustic emission zones, Mathematical Models and Computer Simulations, 19, 59–63, 2007.

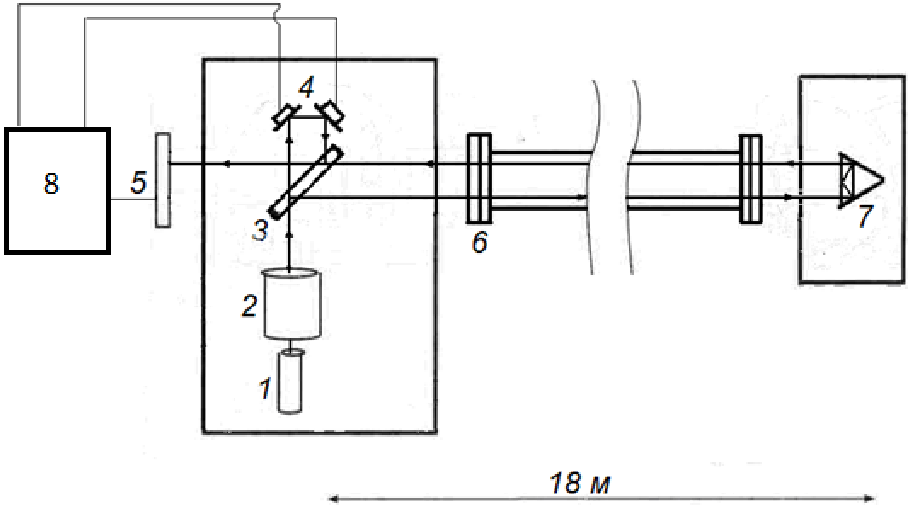

Figure 1. Scheme of a laser strainmeter-interferometer. 1 – He-Ne-laser, 2 – collimator, 3 – flat-parallel plate, 4 – flat-parallel adjustment mirrors, 5 – photodiode, 6 – lightguide, 7 – triple-prism reflector, 8 – registration system block.

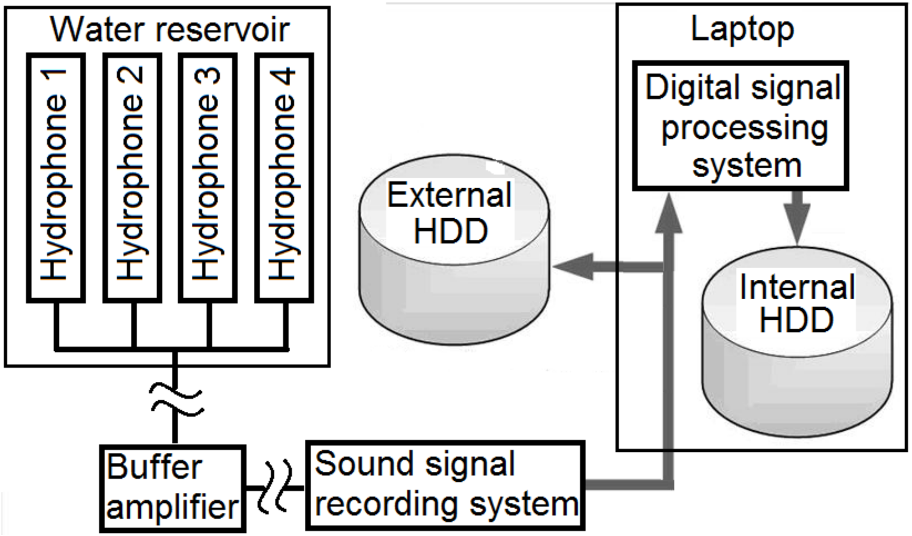

Figure 2. Structural scheme of geoacoustic emission registration system.

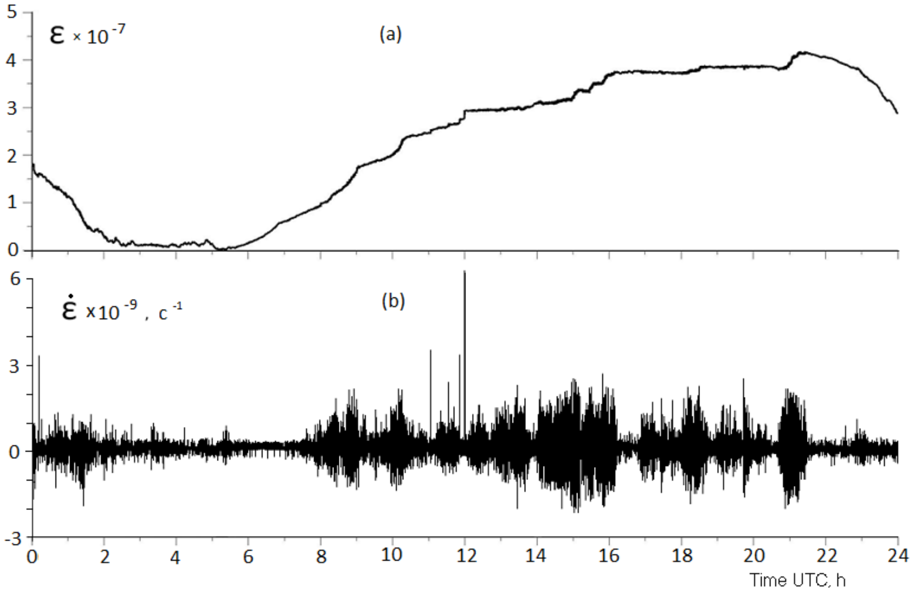

Figure 3. Relative deformation ε **(a)** and its rate $\dot{\varepsilon}$ **(b)** on 9 October 2009.

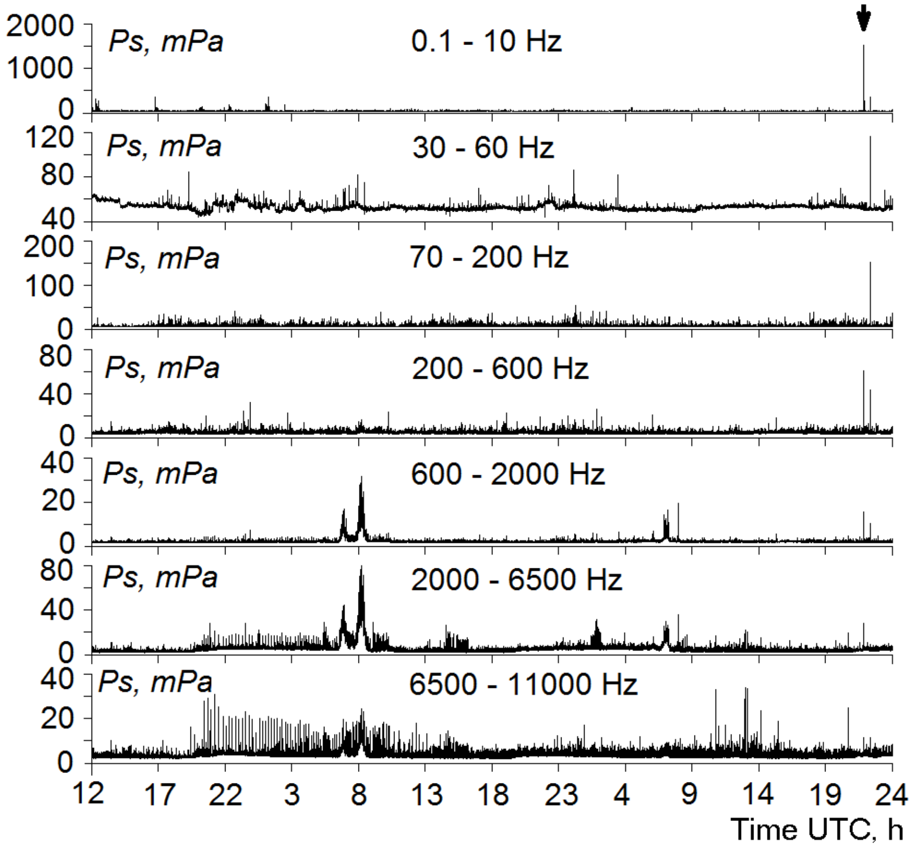

Figure 4. Acoustic emission plots in seven frequency ranges on 22–24 August 2006. The arrow indicates the earthquake at 21:50 UTC.

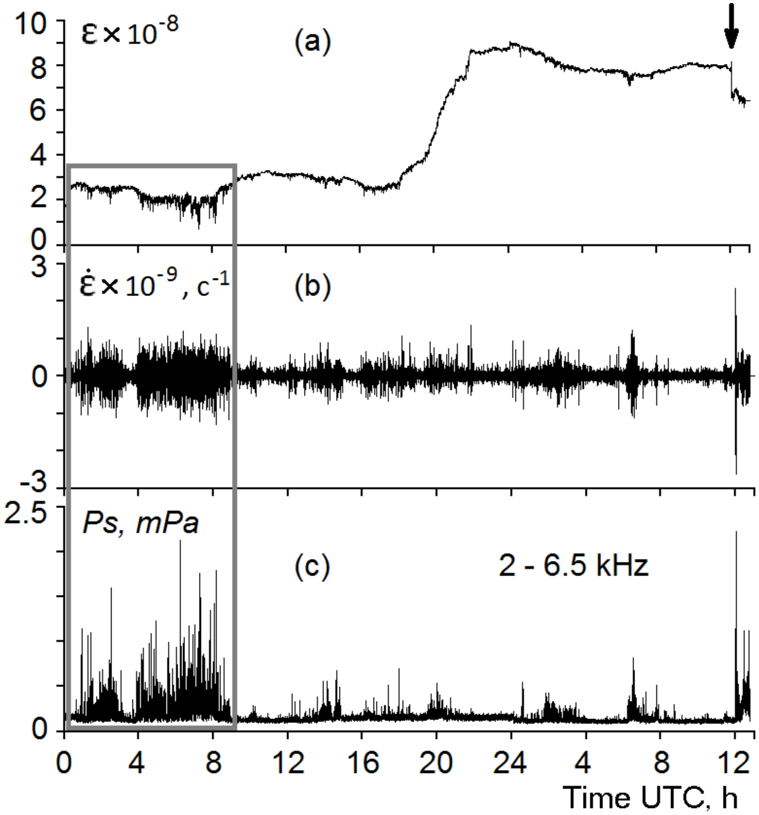

Figure 5. Graphs of relative deformation ε **(a)**, deformation rate $\dot{\varepsilon}$ **(b)**, acoustic pressure P_s **(c)** on 1–2 May 2007. The arrow indicates the earthquake.

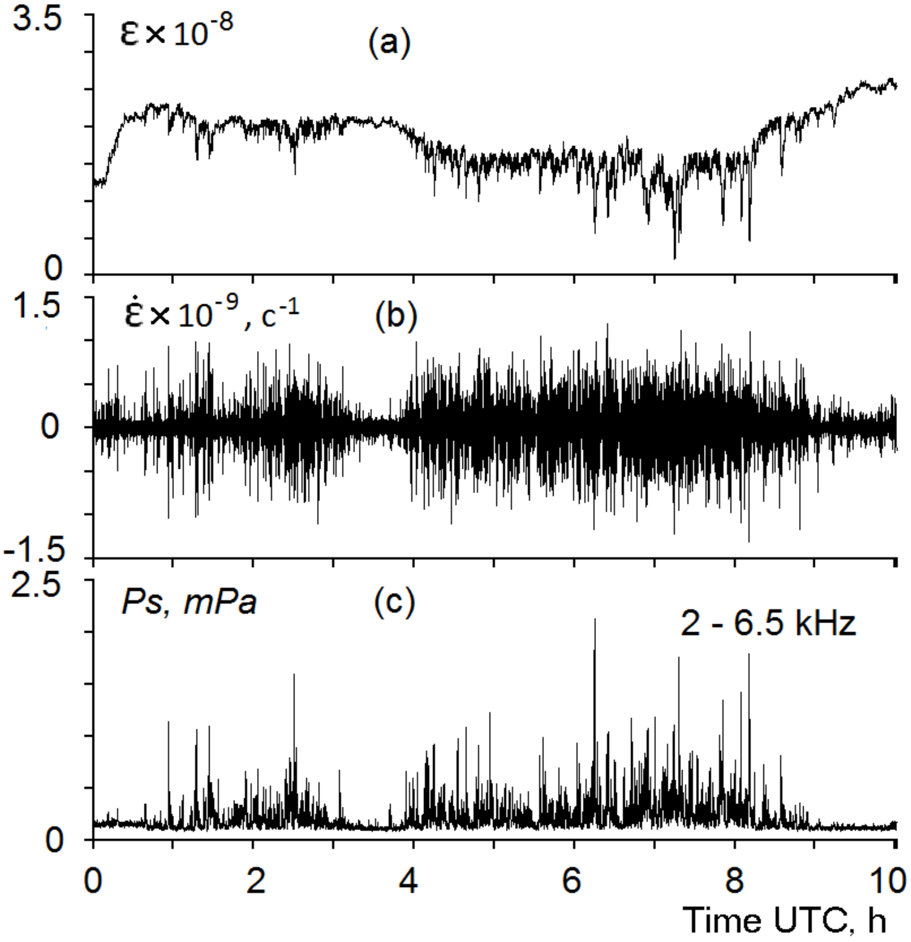

Figure 6. Graph of relative deformation ε **(a)**, its rate $\dot{\varepsilon}$ **(b)** and acoustic pressure P_s **(c)** on 1 May 2007.

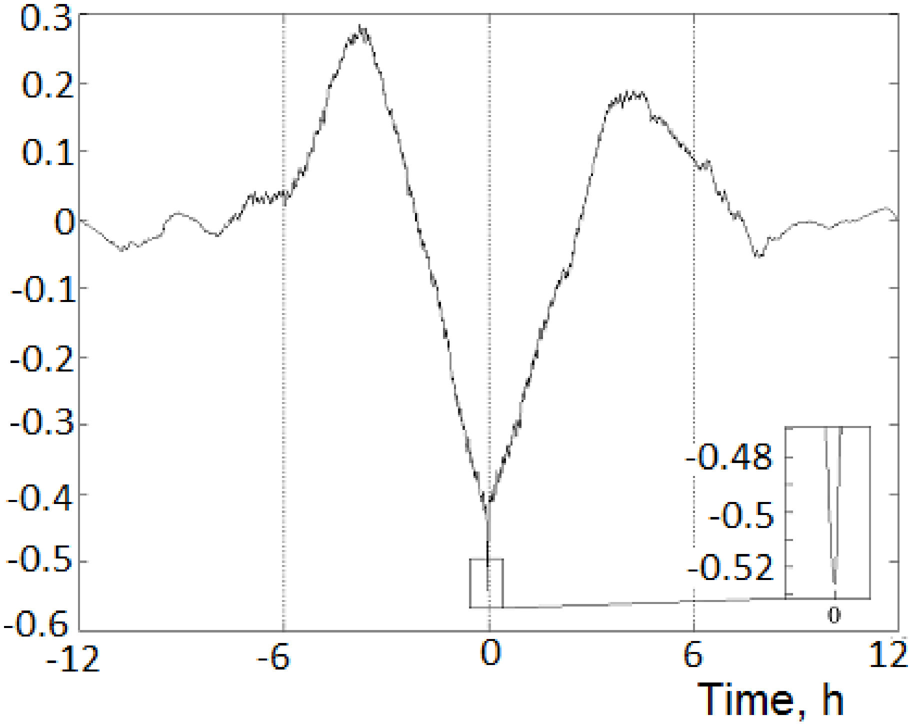

Figure 7. Cross-correlation function graphs between acoustic pressure P_s series in the range of 2.0–6.5 kHz and rock deformations ε.

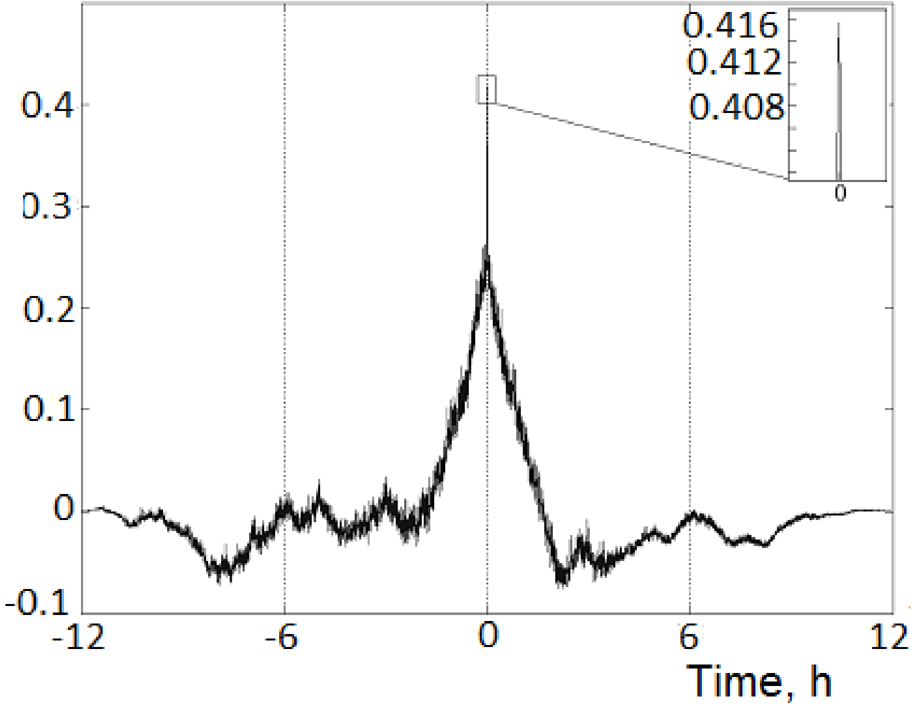

Figure 8. Cross-correlation function graphs between acoustic pressure P_s series in the range of 2.0–6.5 kHz and rock deformation rate $\dot{\varepsilon}$.

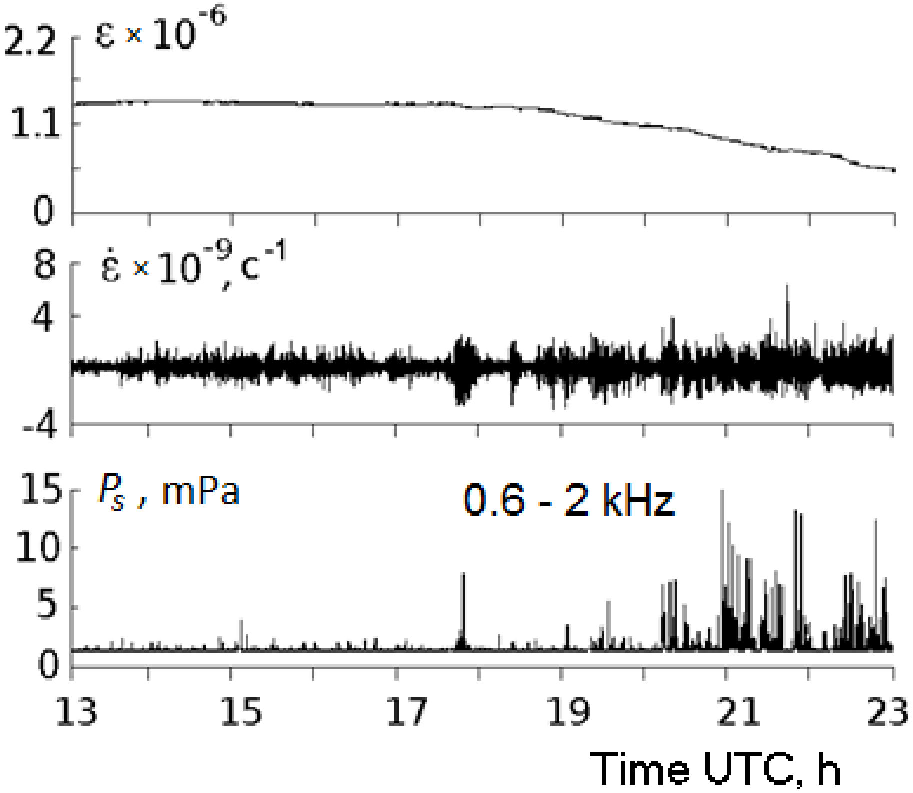

Figure 9. Examples of geoacoustic emission anomalies during near surface rock compression: rock relative deformation ε **(a)**, deformation rate $\dot{\varepsilon}$ **(b)**, acoustic pressure P_s **(c)**.

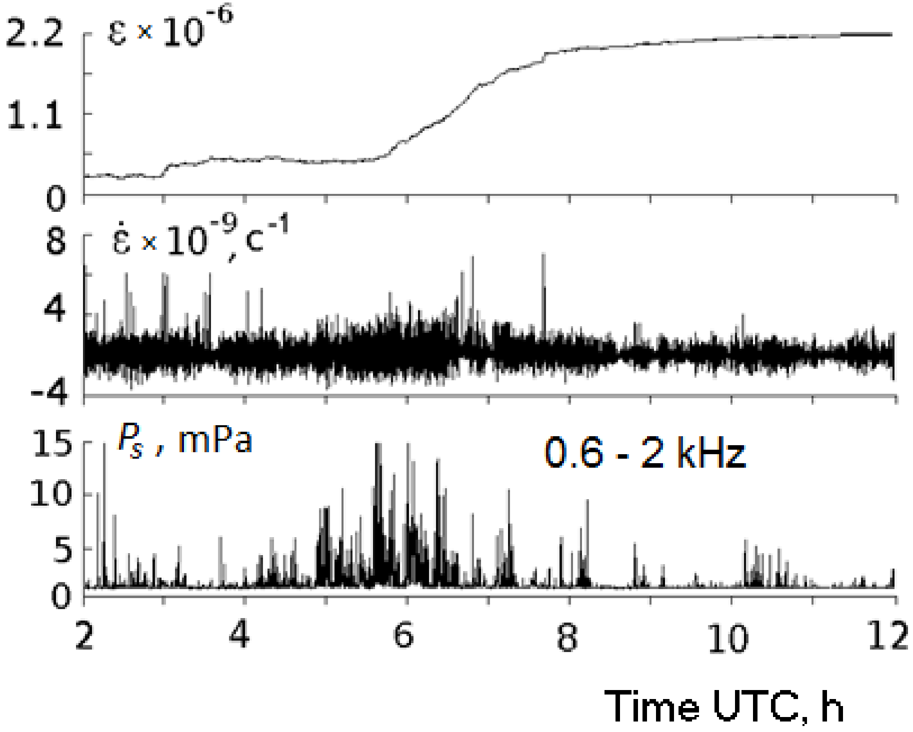

Figure 10. Examples of geoacoustic emission anomaly during near surface rock tension: rock relative deformation ε **(a)**, deformation rate $\dot{\varepsilon}$ **(b)**, acoustic pressure P_s **(c)**.

SED
6, 2401–2422, 2014

Features of the Earth surface deformations in Kamchatka peninsula

I. A. Larionov et al.

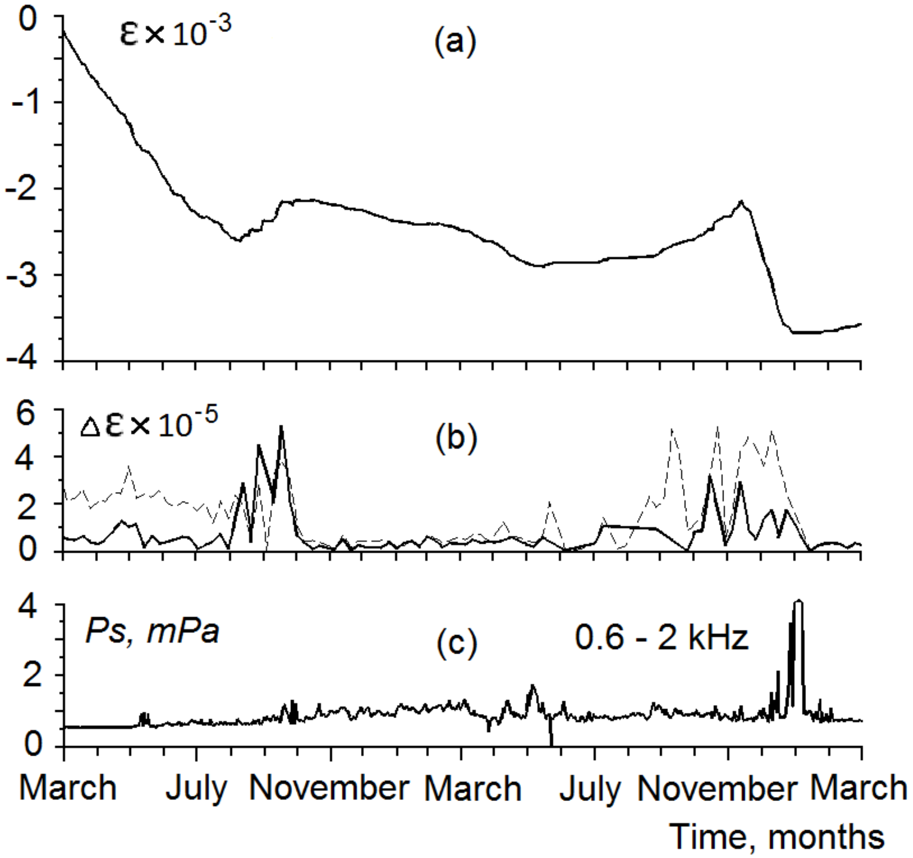

Figure 11. Rock relative deformation ε **(a)**; median values (dashed line) MSD (solid line) of the difference between diurnal relative deformation maximum and minimum values $\Delta\varepsilon$, averaged in a week window **(b)**; acoustic pressure P_s in the range of 0.6–2 kHz, averaged in a day window **(c)** from March 2010 till February 2012.